ELSEVIER

26 September 1994

PHYSICS LETTERS A

Physics Letters A 193 (1994) 126–139

Bubbling of attractors and synchronisation of chaotic oscillators

Peter Ashwin, Jorge Buescu, Ian Stewart

Nonlinear Systems Laboratory, Mathematics Institute, University of Warwick, Coventry CV4 7AL, UK

Received 13 May 1994; revised manuscript received 27 July 1994; accepted for publication 10 August 1994
Communicated by A.P. Fordy

Abstract

We present a system of two coupled identical chaotic electronic circuits that exhibit a blowout bifurcation resulting in loss of stability of the synchronised state. We introduce the concept of *bubbling* of an attractor, a new type of intermittency that is triggered by low levels of noise, and demonstrate numerical and experimental examples of this behaviour. In particular we observe bubbling near the synchronised state of two coupled chaotic oscillators. We give a theoretical description of the behaviour associated with *locally riddled basins*, emphasising the role of invariant measures. In general these are non-unique for a given chaotic attractor, which gives rise to a spectrum of Lyapunov exponents. The behaviour of the attractor depends on the whole spectrum. In particular, bubbling is associated with the loss of stability of an attractor in a dynamically invariant subspace, and is typical in such systems.

1. Introduction

One of the most fundamental questions one can ask about two coupled identical dynamical systems is whether their synchronised (or synchronous) state is stable. It has recently been realised that this question is not as innocuous as it might appear, particularly when the systems are chaotic.

Consider a system of two coupled units governed by an ordinary differential equation of the form

$$\dot{x}_1 = f(x_1) + D(x_2 - x_1),$$

$$\dot{x}_2 = f(x_2) + D(x_1 - x_2),$$

where $x \in \mathbb{R}^m$, $D \in \mathbb{R}$ and such that $\dot{x} = f(x)$ has a chaotic attractor. It is a basic result that the synchronised state $x_1(t) = x_2(t)$ is stable if $D > \frac{1}{2}\lambda$ where λ is the largest Lyapunov exponent for the chaotic state. This is shown by Yamada and Fujisaka [1] for "all-to-all" coupling of a finite number of identical units, while an analogous result for reaction–diffusion equations is found by Pikovsky [2]. Schuster et al. [3] use this property to measure the largest Lyapunov exponent. However, the Lyapunov exponents are quantities that depend in a fundamental way on the choice of an invariant measure on the attractor. Invariant measures are seldom unique. Indeed, usually (for chaotic attractors) there are uncountably many ergodic invariant measures [4].

Pikovsky and Grassberger [5] investigate a system of two coupled tent maps and note that even when a system has a stable synchronised state indicated by the largest Lyapunov exponent, the basin of attraction is densely filled with periodic points; the attractor is surrounded by a strange invariant set which is dense in a neighbourhood of the attractor. They also observe a bifurcation of this attractor to one containing this larger invariant set. They propose that the former attractor can be an attractor only in the weak sense of Milnor [6].

SSDI 0375-9601(94)00669-5

Pecora and Carroll [7] have investigated a related aspect of synchronisation. They split a chaotic system into two subsystems, A and B say. They find that two subsystems B driven by the same system A will typically synchronise only if the Lyapunov exponents of the subsystems (which they refer to as sub-Lyapunov exponents) are negative. De Sousa Vieira et al. [8] study this situation in coupled circle maps and remark that these sub-Lyapunov exponents are Lyapunov exponents of the global system.

The synchronisation problem for identical systems is just one example of a very general situation in which the same issues arise, and it is illuminating to view it in this more general context. The essential ingredients are a dynamical system (for example, defined by a map) on a space M with a dynamically invariant subspace N. Suppose that the restriction of the system to N has an attractor A. The behaviour of the system near A is a combination of the dynamics on A and the dynamics transverse to N (in the synchronisation example, N is the space of synchronised states and the transverse states can be seen as asynchronous perturbations). Because A is an attractor in N, it is stable to perturbations within N. But especially in the case where A is chaotic, the effect of perturbations transverse to N has a global nature that creates room for considerable complexities. Specifically, as the point representing the state of the system moves around near A, it is subjected to different perturbations at different places and it is the combined effect of these that determines the *transverse* stability.

Several authors study such situations; for example Rand et al. [9] examine evolutionary dynamics, where the dynamics is a map on a simplex that maps the boundary components of the simplex (representing zero population levels) to themselves. Kocarev et al. [10] study synchronisation of a pair of identical systems, one driving the other in such a way that the space of synchronised states is invariant (though there need not be any symmetry). Kapitaniak [11] investigates dimensions of attractors for a chain of identical Duffing oscillators coupled sequentially. Alexander et al. [12] examine a map of $\mathbb{R}^2$ with $\mathbb{Z}_3$ cyclic symmetry and find one of the trademarks of such systems, which they name a *riddled basin*. Here an attractor in the invariant subspace can be transversely stable, but the basin of attraction may be a "fat fractal" [13] so that any neighbourhood of the attractor intersects the basin with positive measure, but may also intersect the basin of another attractor with positive measure. This can cause two basins of attraction to be intertwined in a very complex manner.

Subsequently, Ott et al. [14] find that the same behaviour near the invariant subspace can give rise to two different scenarios; either intertwined riddled basins, or a phenomenon recently named *on–off intermittency* by Platt *et al.* [15] where excursions away from the attractor are globally re-injected. Suppose that a parameter that governs the transverse stability of the attractor in the system is varied. Ott et al. define the point at which the largest transverse Lyapunov exponent goes through zero to be a *blowout bifurcation.*

In this paper we shall present some numerical and direct experimental observations of these phenomena as well as reporting theoretical results describing the blowout bifurcation in a general setting. In addition, we discuss a new phenomenon, which we name *bubbling* of an attractor in an invariant subspace. This is a form of noise-driven on–off intermittency that will appear as a precursor to a blowout bifurcation. We demonstrate this behaviour experimentally in the context of synchronisation of chaotic oscillators.

1.1. Terminology

Suppose that A is a compact invariant transitive set for $f : M \to M$. The *basin of attraction* $B(A)$ is the set of points whose ω-limit set is contained in A. Following the ideas of Milnor [6], we say that A is an *asymptotically stable attractor* if it is Lyapunov stable and $B(A)$ contains a neighbourhood of A.

It can happen, however, that although $B(A)$ is large in a measure-theoretical sense and thus we have a positive probability of being attracted to A, it nevertheless contains no open sets. We say that A is a *Milnor attractor* (see Ref. [6]) if it satisfies the weaker condition that $B(A)$ has positive Lebesgue measure. A well-known example of this distinction is the Cantor set of the logistic map at the Feigenbaum point: although Lyapunov stable and attracting a set of full Lebesgue measure, it is not an asymptotically stable attractor. See Ref. [16] for a theoretical explanation of this phenomenon and its implications.

We say that a Milnor attractor A has a *locally riddled basin* if there is an $\epsilon > 0$ such that for every point $x \in$

$B(A)$ any arbitrarily small ball centred on x contains a positive measure set of points whose orbits exceed a distance ϵ from A. This generalises the *riddled basin* attractor defined by Alexander et al. [12] to include the possibility that $B(A)$ contains an open neighbourhood of A (note, however, that A is not asymptotically stable).

We now define the corresponding concepts for repelling sets. We say that a chaotic invariant set A having a dense orbit is a *chaotic saddle* [17] if there is a neighbourhood U of A such that $B(A) \cap U$ is greater than A but has zero Lebesgue measure. Finally, we say that A is a *normally repelling chaotic saddle* if it is an attractor in the invariant subspace but all points not lying on this subspace eventually leave a neighbourhood of A.

Just as an asymptotically stable attractor is a special case of a Milnor attractor, so a normally repelling chaotic saddle is a special case of a chaotic saddle.

Below we shall in addition assume that A has a natural measure that ideally is a Sinai–Bowen–Ruelle (SBR) measure [4] for $f_{|N}$, that is, it is absolutely continuous on unstable manifolds in N.

1.2. A general mechanism for loss of transverse stability

We present a typical scenario for the loss of stability of an attractor in an invariant subspace. Assume that there is a parameter λ that varies the transverse dynamics without changing the dynamics on the invariant subspace (this is reasonable, for example, for coupled systems where a coupling parameter is varied). Moreover, we assume that the normal exponents vary continously with λ and that A is an asymptotically stable attractor for $f_{|N}$. A typical scenario is that there are three parameter values $\lambda_0 < \lambda_1 < \lambda_2$ such that:

(a) For $\lambda < \lambda_0$ the set A is an asymptotically stable attractor.

(b) For $\lambda_0 < \lambda < \lambda_1$ the set A is an attractor with a locally riddled basin.

(c) For $\lambda_1 < \lambda < \lambda_2$ the set A is a chaotic saddle.

(d) For $\lambda_2 < \lambda$ the set A is a normally repelling chaotic saddle.

These three parameter values $\lambda_0 < \lambda_1 < \lambda_2$ are bifurcation points which correspond respectively to A losing asymptotic stability, undergoing a blowout (as defined by Ott et al. [14,18,19]), and becoming normally repelling. Each of these bifurcations can be seen as supercritical (subcritical) according as it creates nearby invariant sets as λ increases (decreases) through the bifurcation point. If all bifurcations from A are subcritical we refer to the scenario as *hysteretic*; if they are all supercritical, we refer to the scenario as *non-hysteretic*. Of course, it can also be typical to have some bifurcations supercritical and others subcritical but we shall not fully examine all possibilities here.

With the addition of noise for the non-hysteretic case of locally riddled basins, we see behaviour that is a precursor of on–off intermittency; we call this *bubbling*. For the hysteretic case, the addition of noise to the riddled basin attractor means that with probability one, a trajectory will eventually leave a neighbourhood of A. In the non-hysteretic case after the blowout, there will be a nearby attractor with on–off intermittent behaviour.

We interpret the bifurcations as being determined by the transverse Lyapunov exponents for the set of ergodic invariant measures whose support is contained in A. On increasing λ, progressively more of these invariant measures become transversely unstable; the blowout bifurcation occurs where the natural measure becomes unstable. Ott et al. have described this behaviour as being due to large deviations in the Lyapunov exponents; although this is essentially the same explanation, we find it useful to think of the behaviour in the way we have just described.

A more complete description of this work is in preparation [20].

2. Electronic experiments

Consider the circuit of one chaotic oscillator shown in Fig. 1. This three degree of freedom system has non-linearity provided by two diodes and is powered by ±5 V. The circuit has an attracting limit cycle for small values of R which undergoes a period-doubling cascade to chaos, producing a Rössler type attractor for larger values of R. The underlying frequency of the periodic orbit before period doubling is of the order of 700 Hz. Care was taken to ensure that the two units were close to identical.

Coupling is provided by breaking a feedback loop and connecting via a capacitance decade box. The cou-

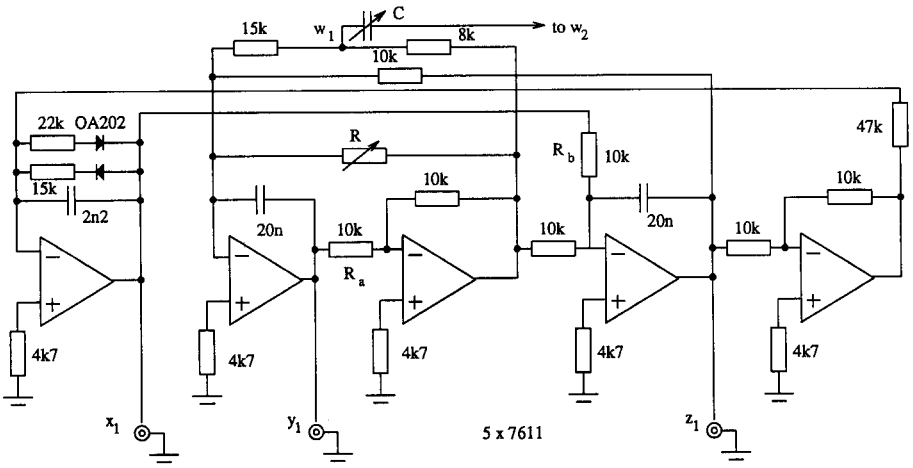

Fig. 1. Circuit diagram of one chaotic oscillator, consisting of three integrators and two inverters with associated feedback components. By varying R it is possible to observe a breakdown to chaos via period doubling of a limit cycle, giving a Rössler-type attractor. Coupling is via the capacitor C.

pling provides an extra degree of freedom, so the coupled system has seven degrees of freedom. Observations in the region of interest show that the asymptotic flow is effectively on a four-dimensional branched manifold, the product of two Rössler-type attractors. The equations of motion are

$$\dot{x}_1 = z_1/103.4 + f(x_1),$$
$$\dot{y}_1 = \tfrac{1}{20}y_1/R - \tfrac{1}{200}z_1 - \tfrac{1}{300}w_1,$$
$$\dot{z}_1 = -\tfrac{1}{200}x_1 + \tfrac{1}{200}y_1,$$
$$C(\dot{w}_1 - \dot{w}_2) = -\tfrac{1}{15}w_1 - \tfrac{1}{8}(y_1 + w_1),$$

with C measured in nF, and a similar system of equations for the second chaotic oscillator is obtained by permuting the subscripts 1 and 2. The non-linear V–I characteristic of the diodes is modelled by the function $f(x)$. By setting $w = w_1 - w_2$ it is possible to write the combined system as an ordinary differential equation on $\mathbb{R}^7$ by noting that $w_1 = \frac{1}{2}w - \frac{8}{46}(y_1 + y_2)$. As $C \to 0$, the equation for $\dot{w}$ becomes singular, and the system reduces to two uncoupled third order equations.

The action of $\mathbb{Z}_2$ by permutation of the oscillators gives an action on the phase space $\mathbb{R}^7$ that permutes the subscripts and reverses the sign of w. The fixed-point space, or synchronous state, is given by $x_1 = x_2$, $y_1 = y_2$, $z_1 = z_2$, $w = 0$; in the notation of Golubitsky et al. [21] this is $\mathrm{Fix}(\mathbb{Z}_2)$, and it is invariant for the dynamics. In the full equations, the fixed point space has codimension three in the seven dimensional space.

2.1. Experimental results

Both circuits are set to the same chaotic state with $R = 39.5$ kΩ and the coupling capacitance was varied from $C = 0$ pF up to $C = 10$ nF. For low values of the coupling, the lack of synchronisation of the oscillators shows in the (x_1, x_2) plane as seemingly random motion of the trace over a square region. From $C = 30$ pF there is evidence of some degree of synchronisation. This gives way via a reverse cascade of period doublings to a stable periodic orbit at $C = 1100$ pF that is not synchronous. This persists until $C = 1139$ pF, where this behaviour goes unstable to a synchronous chaotic attractor. Decreasing the coupling capacitance by a small amount shows that this in-phase attractor coexists hysteretically with a non-in-phase periodic orbit. For C lower than about 1400 pF, small deviations away from $x_1 = x_2$ (synchronicity) are noticeable at irregular intervals. For C reduced further to about 1090 pF, the in-phase chaotic attractor is observable only as a transient, although it can persist for up to a minute.

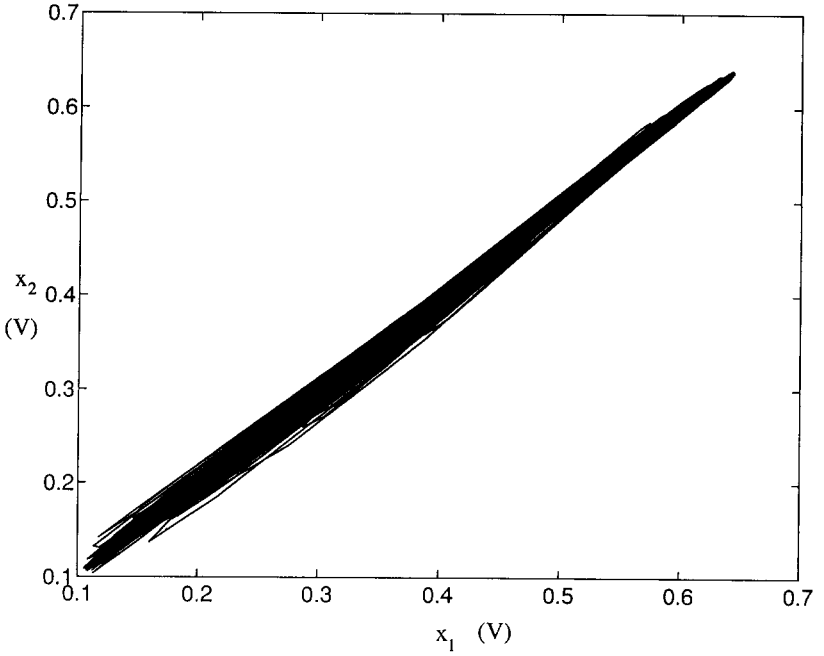

Fig. 2. For $R = 39.5$ kΩ and $C = 1110$ pF, the system evolves towards a state which is close to synchronisation for most of the time, but makes sudden deviations away from it in a seemingly irregular way. Plotted in the (x_1, x_2) plane, the transients going away from the synchronised state are visible deviations of the trajectory from the line $x_1 = x_2$.

3. Analysis of the dynamics

To examine the dynamics of states more closely, we take samples of (x_1, y_1, x_2, y_2) at a rate of 12.5 kHz using a 16-bit A-to-D converter.

For the case of an in-phase attractor exhibiting occasional small excursions from the in-phase subspace, it is possible to reconstruct the dynamics on the symmetric subspace $x_1 = x_2$, $y_1 = y_2$ and approximate the transverse dynamics. Fig. 2 shows a segment of the time series x_1, y_1, x_2, y_2 for the parameter values $R = 39.5$ kΩ and $C = 1110$ pF. Taking a section (interpolating the sample) at $x_1 + x_2 = 1.0$ V we define

$$p = y_1 + y_2, \quad d_x = x_1 - x_2, \quad d_y = y_1 - y_2.$$

Then $d = \sqrt{d_x^2 + d_y^2}$ is the deviation from the fixed point space and $\theta = \tan^{-1}(d_y/d_x)$. The fixed point space of the $\mathbb{Z}_2$-action in this space is given by $d_x = d_y = 0$, that is, the p-axis. The $\mathbb{Z}_2$-action acts as a rotation by π about this fixed-point space.

3.1. Reconstructing the dynamics

Since this is an experiment, we cannot ensure that the two oscillators are exactly identical; we can assume only that the difference between them is small. Thus, we introduce two small numbers, $0 < d_{\min} < d_{\max}$ such that

(i) The fixed-point space is contained within $d < d_{\min}$.

(ii) The behaviour within $d < d_{\min}$ in the p direction is determined by that on the fixed-point space.

(iii) For $d_{\min} < d < d_{\max}$ the behaviour normal to the fixed-point space is dominated by a linear map.

(iv) A significant number of points lie within the range $d_{\min} < d < d_{\max}$.

For the sample in Fig. 2 we pick $d_{\min} = 0.01$ and $d_{\max} = 0.02$. Thus, given the measured return map $(p(n), d_x(n), d_y(n))$ for $n \in \{1 \ldots, N\}$ we plot $p(n+1)$ against $p(n)$ for those n such that $d < d_{\min}$. The return map shown in Fig. 3 is obtained for the sample discussed. The plot includes a fitted sixth order polynomial return map.

We assume that a linear map dominates the be-

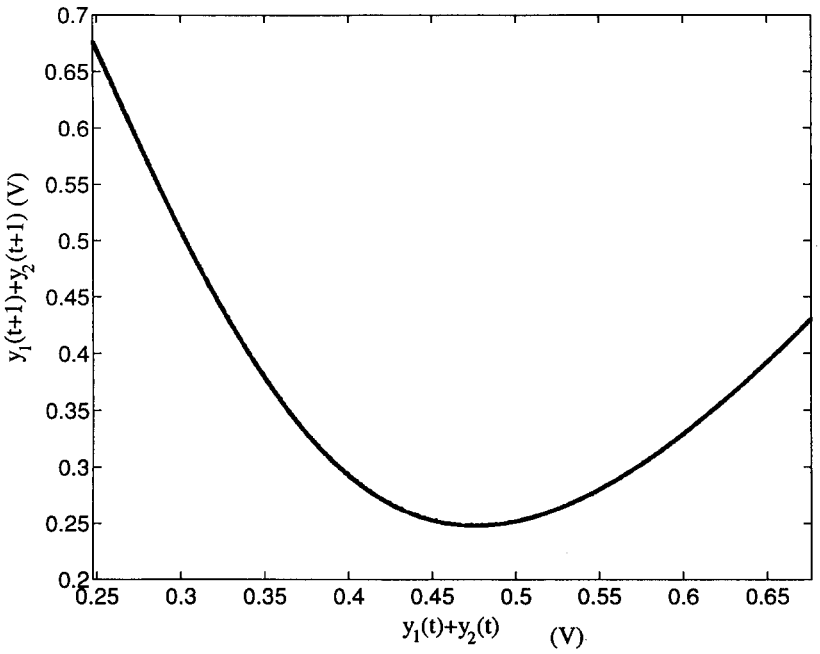

Fig. 3. Return map obtained by interpolating the trajectory shown in Fig. 2 restricting to a tubular neighbourhood of the synchronisation with radius 0.005 V. A sixth order polynomial curve is fitted to this return map; the rms error is 0.47 mV.

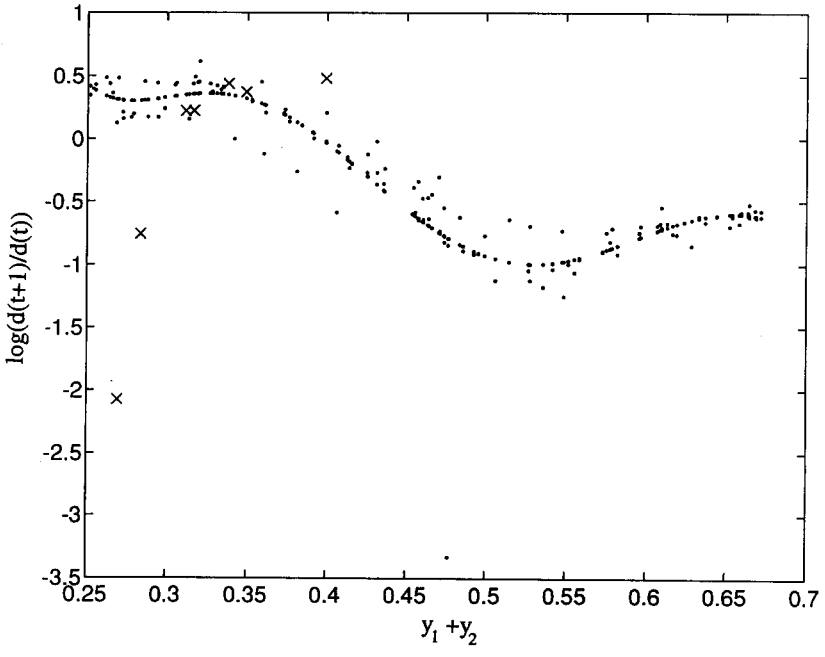

Fig. 4. On the least stable manifold, the points show the logarithm of the ratio of successive returns, that is $\log d(t+1) - \log d(t)$ where t is such that $0.5 < \theta(t) < 2.2$ and $0.005 < d(t) < 0.01$. A positive exponent indicates local repulsion, whereas a negative exponent indicates local attraction. Data are fitted to a sixth order polynomial using a least squares fit. The crosses correspond to samples where $\theta(t)$ is not in the range $0.5 < \theta(t) < 2.2$.

haviour of returns in an annulus $d_{\min} < d < d_{\max}$. For points landing in this annulus, we plot the angle $\theta = \tan^{-1}(d_y/d_x)$ from the plane $d_y = 0$ in the (d_x, d_y) plane. This is observed to be concentrated in one band (modulo π), implying that the dynamics splits into a strongly attracting direction and a marginally stable direction. We concentrate only on those points in the annulus $\theta_{\min} < \theta < \theta_{\max}$ with $\theta_{\min}$ and $\theta_{\max}$ chosen to exclude any outliers. We now make the assumption that the dynamics in this marginally stable direction are determined by the dynamics in the d direction only, and the dynamics here is close to a linear map. Thus, by plotting $\log d(n+1) - \log d(n)$ for n such that $d_{\min} < d(n) < d_{\max}$ and $\theta_{\min} < \theta(n) < \theta_{\max}$, we obtain Fig. 4. We define $\log L$ to be the sixth order polynomial least-squares fit to the local rate of expansion/contraction of d.

3.2. Invariant measures for the reconstructed map

Two types of invariant measure for the interval map on the fixed point space can be easily approximated. These are the natural measure (e.g. SBR measure) and Dirac measures supported on periodic orbits. The natural measure can be obtained by box counting the points which lie within $d < d_{\min}$ in the p direction, to give the measure $\mu_1(y)$. For comparison, we examine the invariant measure obtained from the reconstructed map on the fixed point space. Suppose σ is the standard deviation of the samples in Fig. 3 from the fitted curve $f(p)$. We approximate the natural measure on the fixed point space using the random map $p_{n+1} = f(p_n) + \sigma r$ with r a uniformly distributed random number in the interval $[-1/\sqrt{3}, 1/\sqrt{3}]$ (so that r has zero mean and standard deviation 1). Iterating this random map and box counting using 50 boxes gives the normalised invariant measure $\mu_2(y)$. The measures μ_1 and μ_2 were found to agree well.

The periodic invariant measures were obtained by searching for periodic points of f of low period (up to 6). This was done using a binary chop interval search to locate roots of $f^p(y) - y = 0$.

3.3. Transverse Lyapunov exponents

The normal Lyapunov exponent for the natural measure μ approximated by μ_1 or μ_2 is given by

$$\sigma_{\mathrm{SBR}} = \int_y \log L(y)\, \mathrm{d}\mu(y),$$

while that for the periodic orbit $y_1, \ldots, y_d$ of period d is

$$\sigma_p = \frac{1}{d} \sum_{i=1}^{d} \log L(p_i).$$

Using these formulae, Fig. 5 shows a plot of the various Lyapunov exponents against the supports of the invariant measures. Note that the largest Lyapunov exponent $\sigma_{\max} = 0.277$ is positive and corresponds to Dirac measure on the unique fixed point of the map f. The Lyapunov exponent for both approximations of natural measure, $\sigma^1_{\mathrm{SBR}} = -0.2442$ for μ_1 and $\sigma^2_{\mathrm{SBR}} = -0.2304$ for μ_2 are negative, as expected by the observed attractivity of the fixed point space. What is more, there are periodic points (of period less than 6) which have Lyapunov exponents smaller than σ_{SBR}. The smallest is at $\sigma_{\min} = -0.3264$.

We estimate the errors of the measured σ_{SBR} from the true σ'_{SBR} and obtain under certain assumptions on L that $|\sigma^*_{\mathrm{SBR}} - \sigma_{\mathrm{SBR}}| \sim 0.06$. This is rather smaller than the absolute value of the measured σ_{SBR}. A larger source of uncertainty comes from the fit of L itself. There are several sources of error (rms deviation = 0.27 V) from the fitted curve of L; we believe that noise and the breaking of the idealised symmetry by the real system will be the main sources of error.

4. A numerical example

To enable a more detailed analysis of a typical situation, we consider the following three-parameter map of the plane $M = \mathbb{R}^2$ to itself, which is equivariant under the group $\mathbb{Z}_2$ generated by reflection in the x_1-axis:

$$f_{\alpha,\lambda,\epsilon}\begin{pmatrix} x_1 \\ x_2 \end{pmatrix} = \begin{pmatrix} \frac{3}{2}\sqrt{3}x_1(x_1^2 - 1) + \epsilon x_1^2 x_2 \\ \lambda\, \mathrm{e}^{-\alpha x_1^2} x_2 + x_2^3 \end{pmatrix}. \quad (1)$$

Another closely related map that has the same local behaviour but different global behaviour is defined by

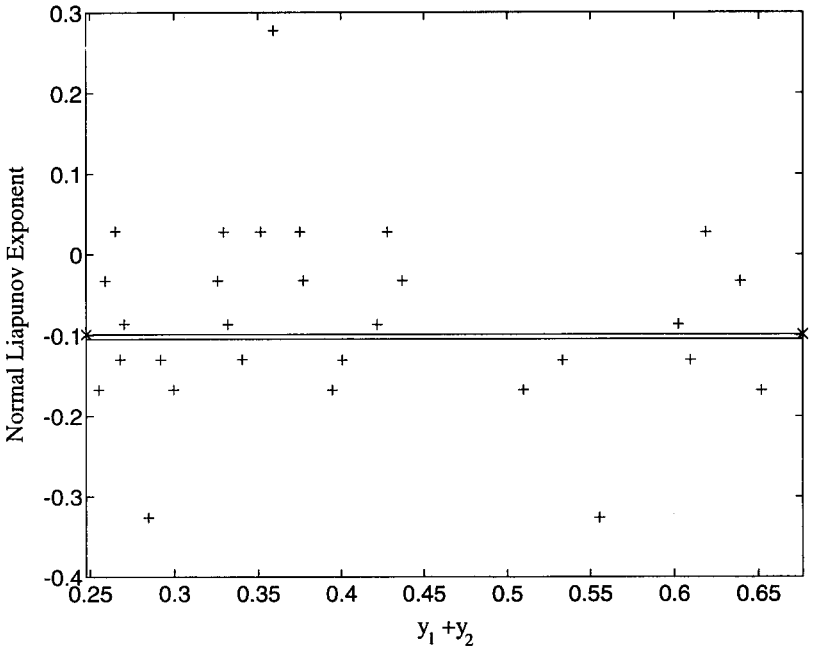

Fig. 5. The normal Lyapunov exponents calculated for the two approximations of the natural invariant measure, and Dirac measures supported on periodic orbits. The horizontal line ending in "×" is the normal Lyapunov exponent for μ_2, while that without "×" corresponds to μ_1. Note that $\sigma_{\max} > 0 > \sigma_{\mathrm{SBR}} > \sigma_{\min}$, indicating that the bubbling scenario discussed in Section 5 can be applied to explain the deviations away from the synchronised state.

$$g_{\alpha,\lambda,\epsilon}\begin{pmatrix} x_1 \\ x_2 \end{pmatrix} = \begin{pmatrix} \frac{3}{2}\sqrt{3}x_1(x_1^2-1) + \epsilon x_1^2 x_2 \\ \lambda\, \mathrm{e}^{-\alpha x_1^2 - x_2^2} x_2 + \frac{1}{2}(1-\mathrm{e}^{-x_2^2})x_2 \end{pmatrix}. \tag{2}$$

Note that the linearisations coincide on $N = \mathbb{R}\times\{0\}$; $\mathrm{D}f(x_1,0) = \mathrm{D}g(x_1,0)$. Without loss of generality, we shall fix $\alpha = 0.7$. The parameter λ is a bifurcation parameter, while for $\epsilon \neq 0$ the vertical foliation of the invariant subspace N is broken. We shall fix $\epsilon = 0.5$. The factor $\frac{3}{2}\sqrt{3}$ is chosen so that for $x_2 = 0$, the interval $A = [-1,1]\times\{0\} \subset N$ is an asymptotically stable chaotic attractor for $f_{|N}$. The symmetry forces $N = \mathrm{Fix}(\mathbb{Z}_2)$ to be invariant under both f and g.

There will be one Lyapunov exponent that determines the transverse stability for each ergodic invariant measure μ supported on A, and this is

$$\sigma_\mu = \int \log\|\mathrm{D}_2 f_2(x_1)\|\,\mathrm{d}\mu(x_1) = \log\lambda - K_\mu\alpha,$$

where

$$K_\mu = \int x_1^2\,\mathrm{d}\mu(x_1).$$

In the case the σ_μ is negative or positive, we say that the measure μ is *transversely stable* or *unstable* respectively.

It follows from a result of Lasota and Yorke [22] that $f_{|N}$ has an ergodic absolutely continuous invariant measure μ_{SBR}; we should expect this measure to play an important role, as it follows from Birkhoff's theorem that for Lebesgue-a.a. x_1 the time average

$$\frac{1}{n}\sum_{j=0}^{n-1}\log|\mathrm{D}_2 f_2 \circ f^j(x_1,0)|$$

converges to σ_{SBR}. For f and g defined as above, the loss of stability of the invariant measures will occur at the same parameter values; these parameter values are shown in Fig. 6.

We claim that f undergoes the hysteretic scenario as λ increases, whereas g undergoes the non-hysteretic scenario described in Section 1.2.

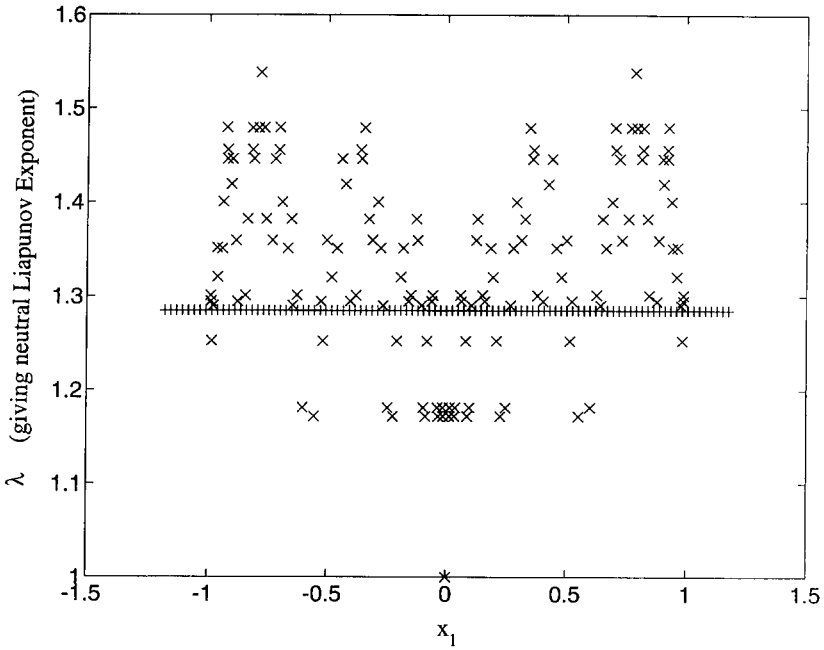

Fig. 6. Values of λ at which various invariant measures lose transverse stability for $\alpha = 0$ for the maps defined by (1) and (2). This is independent of the value of ϵ. On increasing λ, the fixed point at the origin becomes transversely unstable at $\lambda = 0$, the natural measure at $\lambda = 1.285$, and the symmetric period two point at $\lambda = 1.538$.

Turning our attention to f, this has a superstable attractor at infinity. A sequence of pictures showing approximations to the basin of attraction of A are shown in Fig. 7. For $0 < \lambda < 1$, A is an asymptotically stable attractor. As λ passes through 1, the Dirac measure supported on the fixed point at $(0,0)$ becomes transversely unstable; at each point of the preimage set $(0,0)$ (which is dense in A) there will be a transverse "tongue" of instability.

These tongues give rise to a riddled basin of attraction. However, note that the illustrated approximation of $B(A)$ for $\lambda = 1.18$ does not appear to be riddled because the tongues are too narrow to be drawn by the software; only when $\lambda = 1.28$ can we see some fine structure in $B(A)$. At $\lambda = 1.285$ we compute that $\sigma_{\mathrm{SBR}} = 0$ and so there is a blowout bifurcation at this point. For $\lambda = 1.5$, A is a chaotic saddle; the Lebesgue measure of $B(A)$ has gone to zero. There is no sudden jump associated with the loss of Lyapunov stability. What is more, the Lebesgue measure of the basin of A seems to vary continuously with the parameter, even though infinitely many ergodic measures lose transverse stability between $\lambda = 0$ and $\lambda = 1.538$.

In Figs. 8a–8c we show some of the attractors for the map g calculated at various parameter values. For $\lambda < 1.285$ we see an attractor supported on A after transients have died away. For $\lambda > 1.285$, the attractor bifurcates via a non-hysteretic blowout bifurcation to one with a much larger ω-limit set but with a measure close (in the weak sense) to the natural measure on A. By including small additive noise we obtain in Fig. 8d an example of a bubbling state; note that without noise, A is a locally riddled basin attractor.

5. Bubbling and loss of transverse stability

We now report on the theoretical results which support the scenarios presented in Section 1. Rigorous proofs are derived in another work [20] which provides the formal basis for this discussion. Throughout this discussion, M and N are Riemannian manifolds of dimension m and n respectively (with $n < m$) and A is a (compact) asymptotically stable attractor for the restriction $g = f_{|N} : N \to N$.

The Riemannian structure of M and invariance of

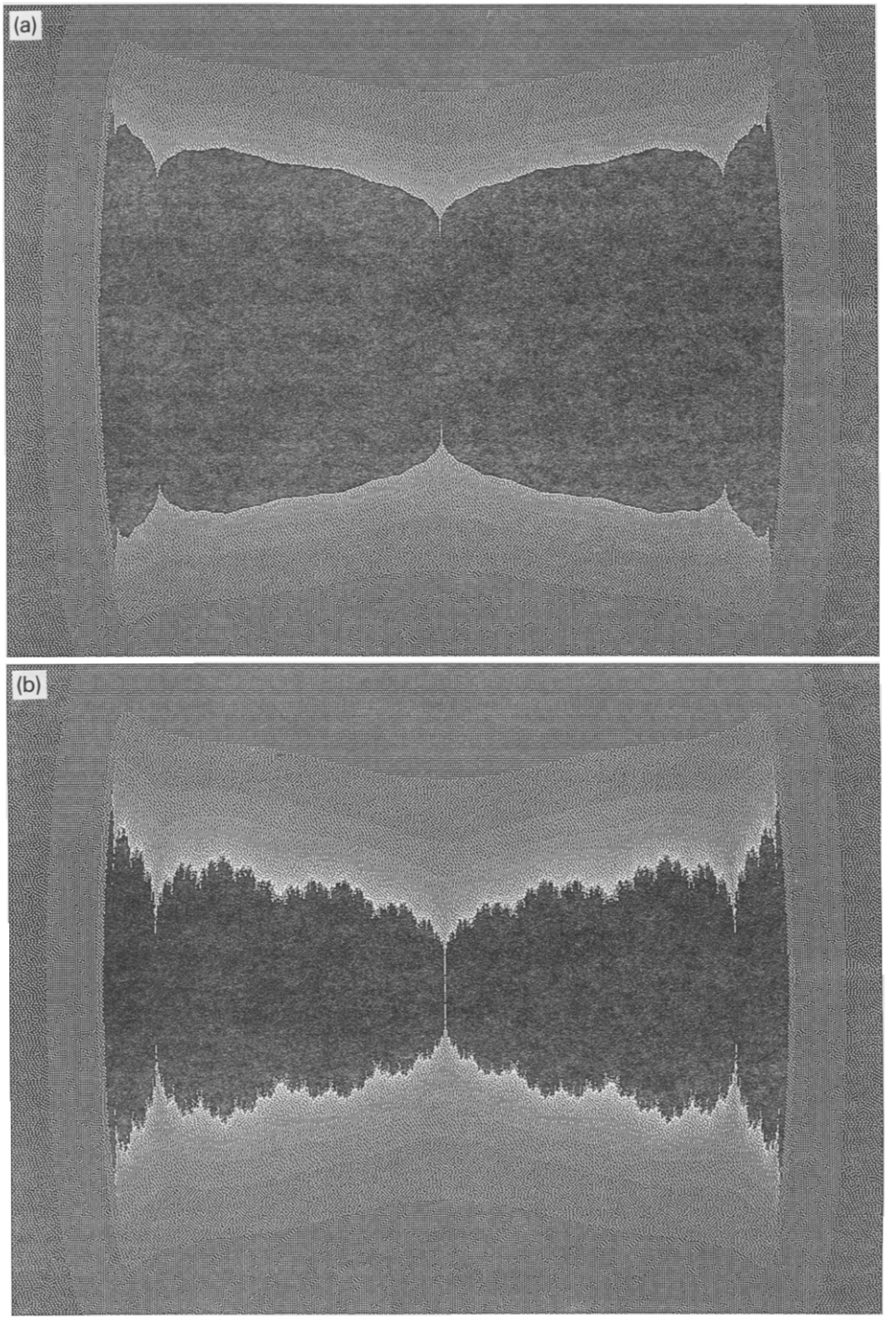

Fig. 7. Basins of attraction for the attractor $A = [-1, 1] \times \{0\}$ under the map $f_{\alpha,\lambda,\epsilon}$ defined in (1). In all cases, the rectangle $[-1.5, 1.5] \times [-1.1, 1.1]$ is shown and the black areas correspond to $B(A)$. The grey areas indicate the basin of attraction of the point at infinity. The parameters are $\alpha = 0.5$, $\epsilon = 0.5$ and (a) $\lambda = 0.9$, with A a Lyapunov-stable attractor. (b) $\lambda = 1.18$, A is a riddled basin attractor; however, this cannot be seen due to $B(A)$ having almost full measure near A. (c) $\lambda = 1.28$, the complex nature of the basin is now more apparent; at $\lambda = 1.285$, there is a hysteretic blowout bifurcation of A. (d) $\lambda = 1.48$, A is a chaotic saddle; however, there is still a set of zero measure that is attracted to A.

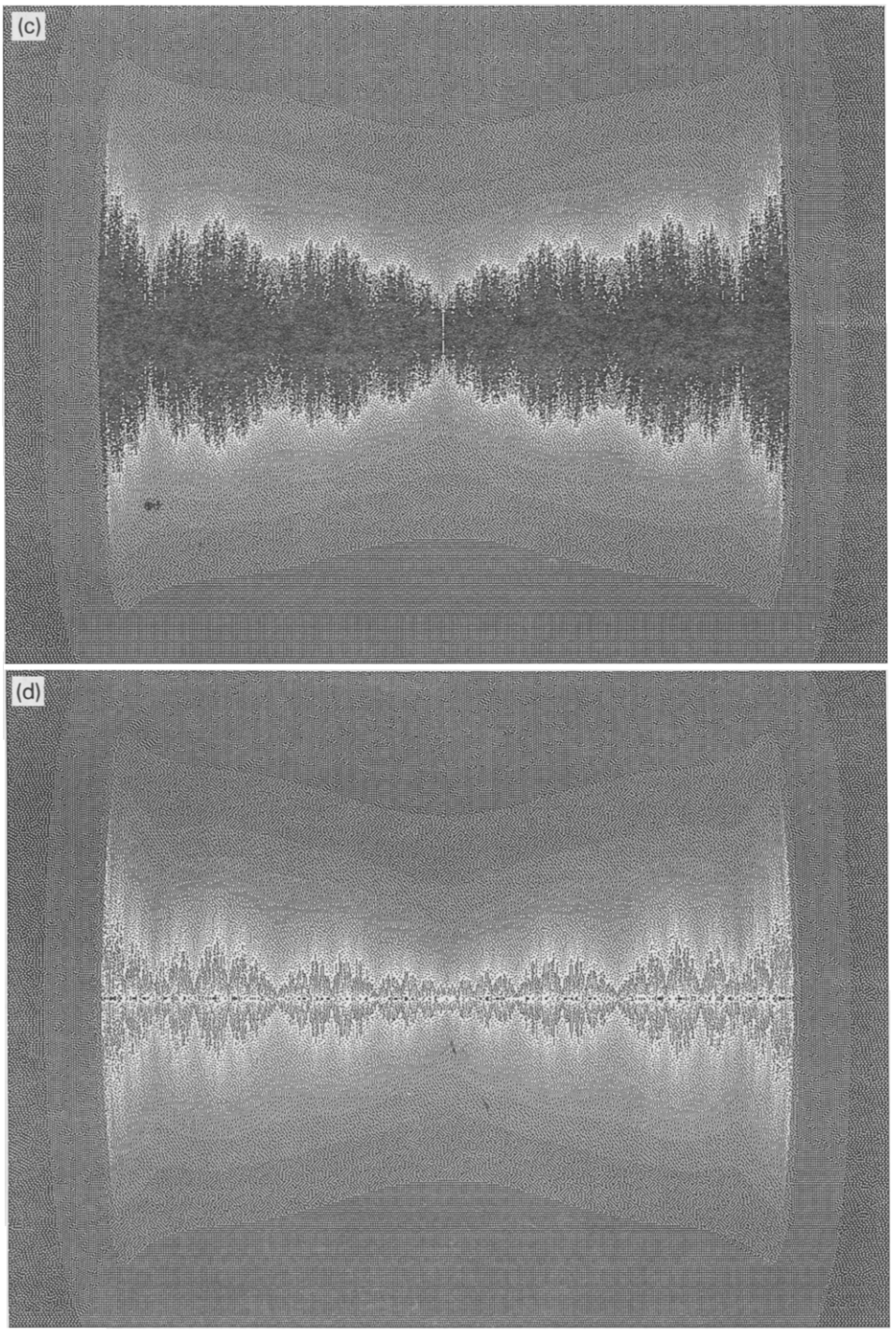

Fig. 7. Continued.

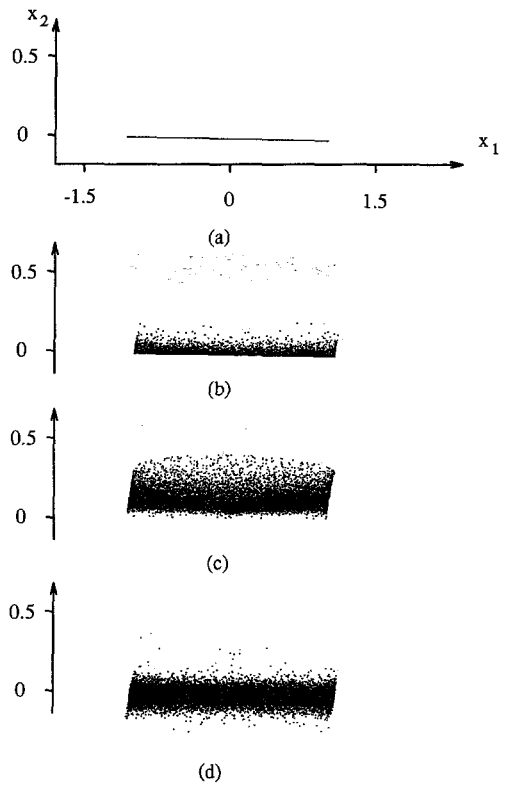

Fig. 8. Observed attractor (for an initial condition starting in the upper half plane) for the map $g_{\alpha,\lambda,\epsilon}$ defined in (2). The black dots show the orbit of one initial point after the transient has died away. The parameters are $\alpha = 0.5$, $\epsilon = 0.5$, (a) $\lambda = 1.18$: the attractor A on the x_1-axis is transversely stable with a locally riddled basin. (b) $\lambda = 1.3$: A has become unstable at $\lambda = 1.285$ and there is now an attracting set with dimension close to two. (c) $\lambda = 1.4$: the attractor moves further from the invariant subspace as it becomes more unstable. (d) As in (a)–(c), but now adding a noisy forcing term uniformly distributed in $[-\eta, \eta]$. In the case where $\alpha = 0.7$, $\epsilon = 0.5$ and $\lambda = 1.2$, we show 50000 iterates after transients have died away. For $\eta = 0.05$ the trajectory performs excursions away from the fixed point space, large compared with the amplitude of the noise. This is an example of bubbling of a stable attractor.

N jointly imply, by an application of Oseledec's multiplicative ergodic theorem, that for any regular point $x \in A$ (that is, such that the Lyapunov exponents at x are defined) the m Lyapunov exponents split into two classes: the n *tangential* exponents (that is, the vectors correspond to directions tangent to N at x) and the $m-n$ *normal* exponents (for those vectors normal to N at x). Moreover, as is to be expected, the tangential Lyapunov exponents coincide with the n Lyapunov exponents at x of the restriction $g = f_{|N} : N \to N$.

The support $\mathrm{supp}(\mu)$ of each ergodic invariant measure μ supported in A is a compact invariant transitive subset of A (that is, it has a dense orbit). By ergodicity, the normal Lyapunov exponents are constant μ – a.e.; denote them by $\lambda_\perp^1(\mu) < \ldots < \lambda_\perp^s(\mu)$. Define the *normal Lyapunov spectrum* $S_n(A)$ as the collection of all the (μ – a.e.) normal exponents for all ergodic invariant measures. Also, define the *stability index* σ_μ of $\mathrm{supp}(\mu)$ as the largest Lyapunov exponent $\lambda_\perp^s(\mu)$.

We suppose that the chaotic attractor A supports an ergodic natural measure μ_{SBR}; this means that, for a set of positive (n-dimensional) Lebesgue measure in the basin of A in N, the time averages converge to the phase averages relative to μ_{SBR}.

The main results proved in Ref. [20] are as follows. First of all, the normal spectrum $S_n(A)$ is bounded above. Secondly, if the normal derivative of f on A (that is, the orthogonal projection of the derivative map of f onto the normal bundle of A) is nonsingular, then the normal spectrum is contained in a compact interval $[s_{\min}, s_{\max}]$. Thirdly, the bounds of the spectrum are also respectively the lim inf and lim sup of the growth rates of the normal derivative for all $x \in A$. So the normal spectrum actually characterises in an optimal way all the possible growth rates of the normal derivative for all $x \in A$.

It then follows by compactness that if $s_{\max} < 0$ or equivalently $\sigma_\mu < 0$ for all invariant measures μ, then A is an asymptotically stable attractor. On the other hand, if $s_{\max} > 0$ then A is Lyapunov unstable. The reason is that by the above characterization of $S_n(A)$ there is at least one invariant transitive subset K of A supporting an ergodic measure with a positive normal exponent; any neighbourhood of A will contain pieces of the μ – a.e. local unstable manifolds, so that points on these unstable manifolds will be repelled away from A.

In general, $s_{\max} \neq \sigma_{\mathrm{SBR}}$. In certain cases (for instance, if x is a periodic orbit) it can be shown by a Hartman–Grobman type of argument that a tongue-shaped open set will be repelled away from A. Thus, if the preimages of x are dense in A, then these tongues will emanate densely from A and the basin of A will be locally riddled.

Thus when $s_{\max}$ crosses 0 on varying a parameter,

the attractor develops a locally riddled basin. Note that the sub- or supercritical nature of this bifurcation depends on the global behaviour: if the local tongues are contained in $B(A)$, we have supercriticality; whereas if there is another attractor whose basin of attraction includes these tongues, we get subcriticality and the attractor has a riddled basin. On adding low level noise in the supercritical case, any trajectory will be forced at some time with probability one to enter an unstable region. It will remain in this tongue with positive probability until it has reached some distance from the attractor; this is the phenomenon of bubbling.

By varying a parameter, increasing numbers of invariant measures lose transverse stability, which increases the local riddling. By a result of Alexander et al. [12] the basin $B(A)$ will have positive measure for $\sigma_{\mathrm{SBR}} < 0$. When $\sigma_{\mathrm{SBR}} > 0$ the m-dimensional Lebesgue measure of $B(A)$ is zero; the set A becomes a chaotic saddle. For $s_{\min} < 0 < \sigma_{\mathrm{SBR}}$ there will be a zero Lebesgue measure set of local stable manifolds to invariant sets in A. This transition is the blowout bifurcation. Depending on the criticality of the bifurcation, either there will be no nearby attractor for $\sigma_{\mathrm{SBR}} > 0$ (subcritical) or there will be on–off intermittency (supercritical) where there is an attractor which makes large deviations away from A but which has most of the natural measure concentrated near A.

Provided that the normal derivative is non-singular, there can be a bifurcation point where $s_{\min}$ crosses zero. This corresponds to the last invariant measure losing transverse stability. By the above characterisation of the spectrum, for all x in A the lim inf of the growth rate of the normal derivative of f is greater than or equal to $s_{\min}$. The non-linear implications of this are that in a neighbourhood of A, the only points that do not iterate away from A lie on the invariant manifold N. This implies that A is a normally repelling chaotic saddle.

We obtain the scenarios described in Section 1.2 by assuming that the map is parametrised by $\lambda \in \mathbb{R}$ and that (i) N is independent of λ, (ii) $f_{|N}$ is independent of λ, and (iii) the transverse instability of A increases monotonically with λ. Note that (i) is naturally satisfied for symmetric systems. In this case the fixed-point spaces are forced to be invariant under the dynamics.

6. Discussion

We see in this situation that the existence of measure-theoretic but not topological attractors arises very naturally. If we assume that the attractor is isolated in the sense of Conley [23], i.e. if it is a chain-transitive component, it cannot have a locally riddled basin. All unstable manifolds must be in the chain-transitive component containing A, so either A is not an attractor, or A is part of a much larger *noisy* attractor $\tilde{A}$. The fact that a neighbourhood of this larger attractor will be explored with probability one for even arbitrarily low noise corresponds to the phenomenon we have named bubbling.

There is an interesting analogy between attractors A with locally riddled basins and heteroclinic cycles (note that these can be structurally stable in symmetric systems [24]). In particular, the ω-limit set of a point attracted to a heteroclinic cycle will be the connected set consisting of the fixed points and their connecting orbits. However, ergodic averages will converge to an invariant measure consisting of Dirac measures supported on the fixed points! In this case, Melbourne [25] has shown that open basins of attraction need not occur. One unsolved problem is whether the ω-limit set will contain the noisy attractor $\tilde{A}$ for a positive measure set of initial conditions.

It is interesting to consider what other invariant sets are created or destroyed as invariant measures on A become unstable. For the map f defined in (1), the periodic points undergo subcritical pitchfork bifurcations; for g defined in (2), the pitchfork bifurcations are supercritical. For $\epsilon = 0$, in both of these maps, there is a vertical foliation making the x_1 dynamics independent of the x_2 dynamics (skew product structure). In this case, the pitchfork bifurcations happen independently of each other and cannot undergo secondary bifurcations. For $\epsilon \neq 0$ it becomes generic to have secondary bifurcations of these periodic points; it would be of interest to examine this case in more detail. One further question that needs to be addressed is the stability of such behaviour to small perturbations that break the invariance of the subspace. Numerical experiments indicate that this structure is stable to small perturbations in an appropriate sense.

Concluding, this investigation shows that we should not expect a chaotic state in an invariant subspace (and in particular a synchronised state of coupled

identical systems) to lose transverse stability at once; a more accurate picture is a "gradual" loss of stability over a range of parameters values. We have presented two natural scenarios for this process.

Acknowledgement

We thank Greg King, Mark Muldoon, David Rand and Peter Walters for helpful conversations. John Marshall helped with the design and construction of the experimental oscillators.

References

[1] T. Yamada and H.Fujisaka, Prog. Theor. Phys. 70 (1983) 1240.
[2] A.S. Pikovsky, Z. Phys. B 55 (1984) 149.
[3] H.G. Schuster, S. Martin, and W. Martienssen, Phys. Rev. A (1986) 3547.
[4] J. P. Eckmann and D. Ruelle, Rev. Mod. Phys. 57 (1985) 617.
[5] A.S. Pikovsky and P. Grassberger, J. Phys. A 24 (1991) 4587.
[6] J. Milnor, Commun. Math. Phys. 99 (1985) 177.
[7] L.M. Pecora and T.L. Carroll, Phys. Rev. Lett. 64 (1990) 821.
[8] M. de Sousa Vieira, A.J. Lichtenberg and M.A. Lieberman, Phys. Rev. A 46 (1992) 7359.
[9] D.A. Rand, H. Wilson and J. McGlade, Dynamics and evolution: evolutionarily stable attractors, invasion exponents and phenotype dynamics, University of Warwick preprint (1992).
[10] L. Kocarev, A. Shang and L.O. Chua, Int. J. Bifurcation Chaos 3 (1993) 479.
[11] T. Kapitaniak, Phys. Rev. E 47 (1993) 2975.
[12] J.C. Alexander, I. Kan, J.A. Yorke and Zhiping You, Int. J. Bifurcation Chaos 2 (1992) 795.
[13] J.D. Farmer, Phys. Rev. Lett 55 (1985) 351.
[14] E. Ott and J.C. Sommerer, Phys. Lett. A 188 (1994) 39.
[15] N. Platt, E.A. Spiegel and C. Tresser, Phys. Rev. Lett. 70 (1993) 279.
[16] J. Buescu and I. Stewart, Ergod. Th. Dynam. Sys., to appear (1994).
[17] H. Nusse and J. A. Yorke, Ergod. Th. Dynam. Syst. 11 (1991) 189.
[18] E. Ott, J.C. Sommerer, J.C. Alexander, I. Kan and J.A. Yorke, Phys. Rev. Lett. 71 (1993) 4134.
[19] E. Ott, J.C. Sommerer, J.C. Alexander, I. Kan and J.A. Yorke, A transition to chaotic attractors with riddled basins, Physica D, to appear (1994).
[20] P. Ashwin, J. Buescu and I.N. Stewart, From attractor to chaotic saddle: a tale of transverse instability, in preparation (1994).
[21] M. Golubitsky, I.N Stewart and D. Schaeffer, Groups and singularities in bifurcation theory, Vol. 2, Appl. Math. Sci., Vol. 69 (Springer, Berlin, 1988).
[22] A. Lasota and J.A. Yorke, Trans. Am. Math. Soc. 186 (1973) 481.
[23] C.C. Conley, Isolated invariant sets and the Morse index, Conf. Board in Math. Sci. 38 (1978).
[24] J. Guckenheimer and P. Holmes, Math. Proc. Cambridge Philos. Soc. 103 (1988) 189.
[25] I. Melbourne, Nonlinearity 4 (1991) 835.